Atomic Ionization by Scalar Dark Matter and Solar Scalars

H. B. Tran Tan,[1,2] A. Derevianko,[1] V. A. Dzuba,[2] and V. V. Flambaum[2,3]
[1]Department of Physics, University of Nevada, Reno, Nevada 89557, USA
[2]School of Physics, University of New South Wales, Sydney 2052, Australia
[3]Helmholtz Institute Mainz, Johannes Gutenberg University, 55099 Mainz, Germany

(Received 18 May 2021; accepted 15 July 2021; published 20 August 2021)

We calculate the cross sections of atomic ionization by absorption of scalar particles in the energy range from a few eV to 100 keV. We consider both nonrelativistic particles (dark matter candidates) and relativistic particles that may be produced inside the Sun. We provide numerical results for atoms relevant for direct dark matter searches (O, Na, Ar, Ca, Ge, I, Xe, W and Tl). We identify a crucial flaw in previous calculations and show that they overestimated the ionization cross sections by several orders of magnitude due to violation of the orthogonality of the bound and continuum electron wave functions. Using our computed cross sections, we interpret the recent data from the Xenon1T experiment, establishing the first direct bounds on coupling of scalars to electrons. We argue that the Xenon1T excess can be explained by the emission of scalars from the Sun. Although our finding is in a similar tension with astrophysical bounds as the solar axion hypothesis, we establish direct limits on scalar DM for the ∼1–10 keV mass range. We also update axio-ionization cross sections. Numerical data files are provided.

DOI: 10.1103/PhysRevLett.127.081301

The nature of dark matter (DM) remains an unsolved problem of modern physics. Current experiments searching for the simplest form of the weakly interacting massive particles (WIMPs) have exhausted their predicted parameter space without obtaining unequivocal signals [1–8]. With experimental tests for supersymmetric theories, which supply WIMP candidates [9–16], also experiencing difficulties, there is a growing interest in other DM candidates, including pseudoscalars (axions and axionlike particles [17–32]) and scalars. In particular, the intriguing excess rate in the recent Xenon1T experiment [33] was attributed to solar axions (at the 3.5σ level). Although this interpretation remains in tension with astrophysical bounds [34], here we examine if the scalar particles could account for the observed Xenon1T excess. Not only do we show that the previous work [35] substantially overestimated the cross sections of atomic ionization by scalars and provide cross section data for a variety of detectors, we also demonstrate that the Xenon1T excess can be explained by the emission of scalars from the Sun. Our finding is in a similar tension with astrophysical bounds as the solar axion hypothesis; however, we establish direct limits on scalar DM for the ∼1–10 keV mass range.

Examples of scalars are abundant and include the scalar familon, the sgoldstino, the dilaton, the relaxon, moduli, and Higgs-portal DM. Among these, the Higgs-portal scalar DM has become particularly well motivated since the discovery of the Higgs particle at the Large Hadron Collider [36]. Detection techniques for ultralight DM scalars of mass $m \ll 1$ eV rely on a variety of techniques: atomic clocks [37–42], resonant-mass detectors [43], accelerometers [44], atomic gravitational wave detectors [45], laser and maser interferometry [39,46–48], atom interferometers [49], pulsar timing, and nongravitational lensing [50]. Interactions between heavier scalars and electrons can drive detectable bound-bound transitions in atomic and molecular systems [51] if their energies match the transition frequencies. Here we focus on DM scalars of mass $m \sim O(\mathrm{keV})$ that can drive bound-continuum transitions, leading to ionization of atoms. This ionization channel contributes to the detection rates of DM particle detectors. Because DM halo particles are nonrelativistic, ultralight DM scalar candidates cannot be probed directly in particle detectors because of their small energies. Nevertheless, these detectors may be sensitive to the fluxes of ultralight scalars produced in the Sun. Solar scalars may have enough energy to ionize the detector's atoms, leading to measurable signals.

In this Letter we consider the ionization of atoms by scalar particles. This process was considered alongside the axioelectric effect in an attempt to explain the signal modulation observed by DAMA/NaI [35]. It was later pointed out that Bernabei *et al.* [35] underestimated the axioelectric effects by several orders of magnitude due to

the omission of the leading term in the axion-electron Hamiltonian [52]. Here, we show that Bernabei *et al.* [35] overestimated the scalar ionization process by several orders of magnitude due to the use of electron plane waves that do not obey orthogonality conditions to electron bound states. Furthermore, the calculation in Ref. [35] used a simple model of atoms that ignored relativistic and many-body effects. As a result, a relativistic Hartree-Fock (HF) atomic calculation of the ionization cross section is needed and is performed, for the first time, in this Letter. The results of this work may be used in experiments searching for DM and solar particles using underground detectors.

Theory.—The Lagrangian density of a scalar field ϕ coupled to an electron field ψ may be written in the form

$$\mathcal{L}_{\phi\bar{e}e} = \sqrt{\hbar c}\, g_{\phi\bar{e}e}\phi\bar{\psi}\psi, \tag{1}$$

where $g_{\phi ee}$ is a dimensionless coupling constant. We consider the ionization process in which an atomic electron in the bound state absorbs a scalar particle ϕ with energy ϵ and is ejected into the continuum. The ionization cross section may be written in the form

$$\sigma_\phi = g^2_{\phi\bar{e}e}(c/v)Q(\epsilon)a_0^2, \tag{2}$$

where c is the speed of light, v is the scalar particle's velocity in the laboratory frame, and $a_0 \approx 5.29 \times 10^{-11}$ m is the Bohr radius. In standard halo models of nonrelativistic DM, a typical velocity is $v \sim 10^{-3}c$. We also consider the case of ultrarelativistic scalars, which may be produced in the solar interior. Therefore, in addition to the nonrelativistic scalar case, we performed calculations for $m = 0$. All intermediate cases are between the curves for the nonrelativistic case and $m = 0$ case in the graphs in Fig. 2.

The dimensionless form factor $Q(\epsilon)$ may be presented as a multipolar expansion (see the Supplemental Material [53] for a derivation)

$$Q(\epsilon) = \frac{\pi\hbar^2c^2}{\epsilon a_0^2}\sum_{bc}\sum_{L=0}^{\infty}(2L+1)|\langle b||\upsilon_L||c\rangle|^2, \tag{3}$$

where the reduced matrix element $\langle b||\upsilon_L||c\rangle$ is given by

$$\begin{aligned}\langle b||\upsilon_L||c\rangle = {} & (-1)^{j_b-1/2}\sqrt{(2j_b+1)(2j_c+1)} \\ & \times \begin{pmatrix} j_b & j_c & L \\ -1/2 & 1/2 & 0 \end{pmatrix}\Pi(l_b+L+l_c) \\ & \times \int (f^{\kappa_b}_{\epsilon_b}f^{\kappa_c}_{\epsilon_c} - \alpha^2 g^{\kappa_b}_{\epsilon_b}g^{\kappa_c}_{\epsilon_c})j_L(kr)dr. \end{aligned} \tag{4}$$

Here, the functions f and g are the upper and lower radial components of the electron wave function

$$\psi(\mathbf{r}) = \frac{1}{r}\begin{pmatrix} f^\kappa_\epsilon(r)\Omega^\kappa_m \\ i\alpha g^\kappa_\epsilon(r)\Omega^{-\kappa}_m \end{pmatrix}, \tag{5}$$

where α is the fine structure constant, ϵ_b is the electronic bound state's energy, j_b its total angular momentum, l_b its orbital angular momentum, and $\kappa_b \equiv (j_b + 1/2)(-1)^{l_b+1}$. The quantities ϵ_c, j_c, l_c, and κ_c are similarly defined for the continuum state. We assumed that the bound state wave functions are normalized to unity whereas the continuum wave functions are normalized to the δ function of energy $\delta(\epsilon_c - \epsilon'_c)$. Note that the continuum state energy necessarily satisfies the energy conservation condition $\epsilon_c = \epsilon_b + \epsilon$. The function $\Pi(x)$ imposes parity selection rules; it returns 1 if x is even and zero if x is odd. The quantity $k = \sqrt{(\epsilon/c)^2 - (mc)^2}/\hbar = \epsilon v/(\hbar c^2)$ is the wave number of the scalar particle and $j_L(\ldots)$ is the spherical Bessel function of order L. The summation over L saturates very rapidly and we cut it at $L = 3$. The electronic bound and continuum wave functions needed for the radial integral in Eq. (4) are calculated using the relativistic HF method. The HF energies of all core states for several atoms of interest may be found in the Supplemental Material [53].

It is worth emphasizing the failure of the photoionization-derived intuition (see, e.g., [54]) about the relative importance of various multipolar contributions to Eq. (3). We find that the monopole $L = 0$ contribution is suppressed due to the following "orthogonality" arguments. The integral in the monopole ($L = 0$) contribution to the matrix element in Eq. (4) may be presented as

$$\begin{aligned}&\int (f^{\kappa_b}_{\epsilon_b}f^{\kappa_c}_{\epsilon_c} - \alpha^2 g^{\kappa_b}_{\epsilon_b}g^{\kappa_c}_{\epsilon_c})j_0(kr)dr \\ &\quad = 2\alpha^2\int g^{\kappa_b}_{\epsilon_b}g^{\kappa_c}_{\epsilon_c}dr \\ &\qquad + \int (f^{\kappa_b}_{\epsilon_b}f^{\kappa_c}_{\epsilon_c} - \alpha^2 g^{\kappa_b}_{\epsilon_b}g^{\kappa_c}_{\epsilon_c})[j_0(kr) - 1]dr, \end{aligned} \tag{6}$$

where we have used the orthogonality condition between the bound and continuum radial wave functions, $\int (f^{\kappa_b}_{\epsilon_b}f^{\kappa_c}_{\epsilon_c} + \alpha^2 g^{\kappa_b}_{\epsilon_b}g^{\kappa_c}_{\epsilon_c})dr = 0$. In the nonrelativistic approximation, the first term on the right-hand side of Eq. (6) vanishes and the second term is small because $|j_0(kr) - 1| \approx (kr)^2/6$. For massive nonrelativistic scalar $kr \approx 0$. For massless scalar, $kr \ll 1$ in the interested energy range.

Bernabei *et al.* [35] calculated the integral in Eq. (6) in the nonrelativistic electron limit and obtained a nonzero result when $j_0(kr) \approx 1$. This is because they used, for the outgoing electron, plane waves instead of proper continuum wave functions, violating the orthogonality condition. As a result, Bernabei *et al.* [35] strongly overestimated the cross section. In Fig. 1, we show the results of computing the form factor $Q(\epsilon)$ for the ionization

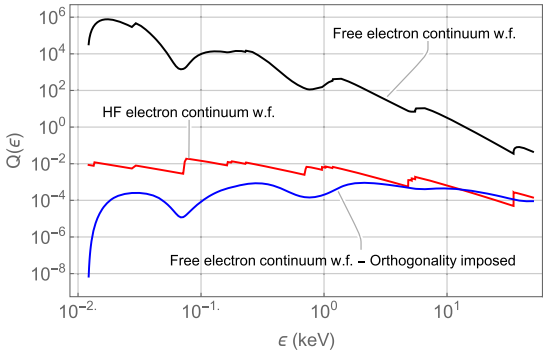

FIG. 1. Comparison of the form factor $Q(\epsilon)$ for ionization of Xe by massive scalars obtained by using a HF continuum wave function (red line), a free continuum wave function (black line), and a free continuum wave function with an orthogonality condition imposed (blue line).

of Xe by massive scalars using (a) a HF continuum wave function, (b) a free continuum wave function, and (c) a free continuum wave function with orthogonality condition enforced manually. It is clear that the naive use of a free continuum wave function gives incorrect results [55].

The next order term with $L = 1$ in Eq. (4) is proportional to $\int f^{\kappa_b}_{\epsilon_b} f^{\kappa_c}_{\epsilon_c} r dr$, which is the same as the radial integral appearing in the photoionization cross section σ_γ. For ultrarelativistic scalars, this $L = 1$ term dominates over the small $L = 0$ term and one has (see the Supplemental Material [53]).

$$\sigma_\phi(m = 0)/\sigma_\gamma(\epsilon_\gamma = \epsilon) \approx g^2_{\phi\bar{e}e}/(4\pi\alpha). \tag{7}$$

On the other hand, for massive scalars, the $L = 1$ contribution is suppressed, compared to its massless counterpart, by the factor $v/c \approx 10^{-3}$,

$$\sigma^{L=1}_\phi(mc^2 \approx \epsilon)/\sigma_\gamma(\epsilon_\gamma = \epsilon) \approx g^2_{\phi\bar{e}e} v/(4\pi\alpha c). \tag{8}$$

This suppression factor makes the massive $L = 1$ term somewhat smaller than the massive $L = 0$ term.

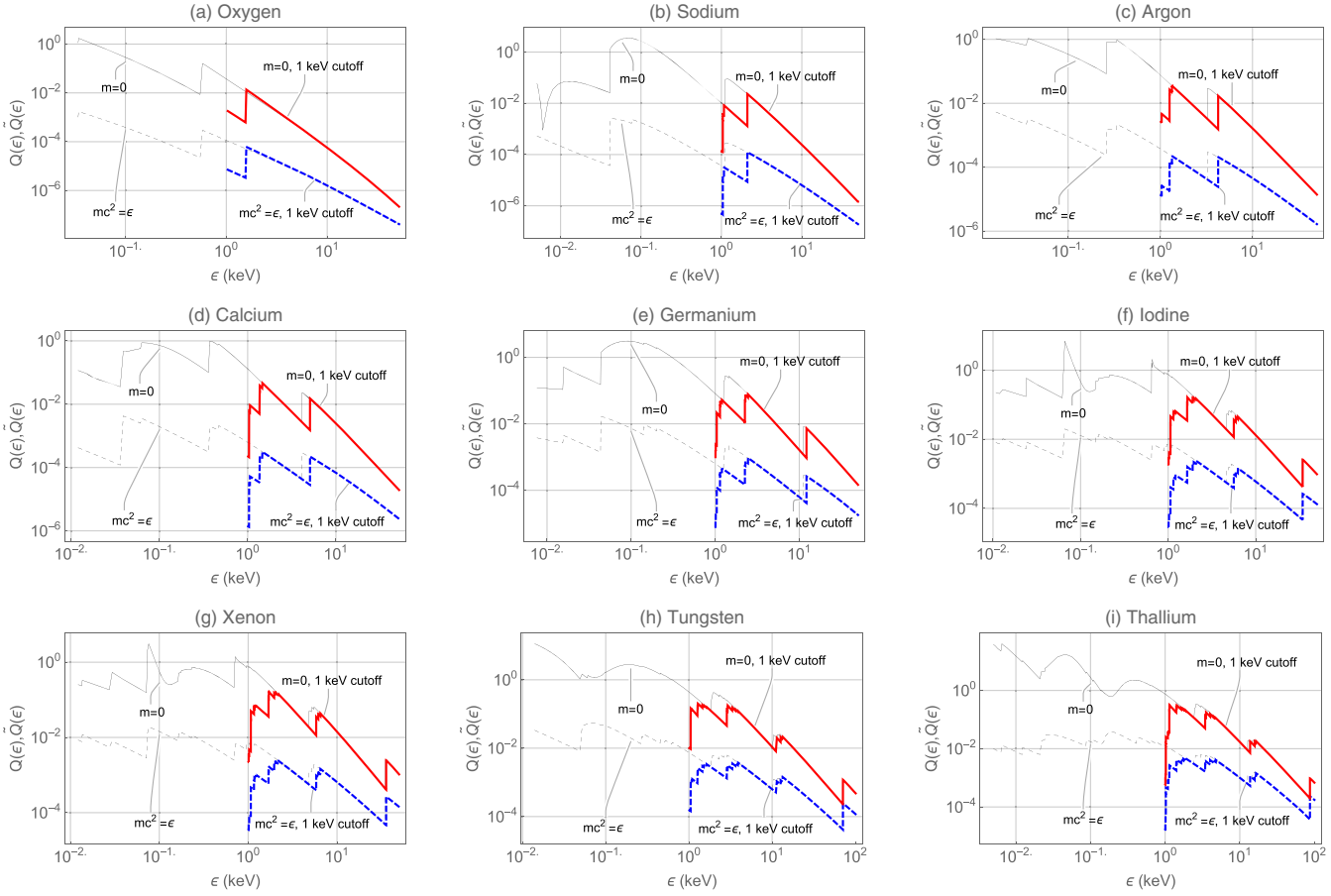

FIG. 2. Dimensionless form factors in the ionization cross sections of O, Na, Ar, Ca, Ge, I, Xe, W and Tl by scalar particles of mass m and energy ϵ. Thin black line, Q for $m = 0$; thin dashed black line, Q for $mc^2 = \epsilon$; thick red line, $\tilde{Q}$ for $m = 0$; thick dashed blue line, $\tilde{Q}$ for $mc^2 = \epsilon$. The leftmost sides of the graphs correspond with the lowest energies that can excite an electron. For all energies smaller than these, the factors Q and $\tilde{Q}$ have value zero. The numerical data used to plot these graphs and others are presented in the Supplemental Material [53].

Using Eq. (7) and experimental data on photoionization cross sections [57–59], we performed a test for our numerical calculations, obtaining agreement within a few percent accuracy, except for near the thresholds of ionization, where the difference is about 10%.

Results.—We computed the form factor $Q(\epsilon)$ in the expression for the ionization cross section (2) for several atoms currently used in DM search experiments including O, Na, Ar, Ca, Ge, I, Xe, W and Tl [2–5,24,33,60–67]. The results are presented in Fig. 2. In our calculations, correlation corrections and field-theoretic effects beyond the relativistic HF approximation are ignored. The accuracy of this approximation is a few percent due to the dominating contribution from the inner core states. For these states the correlation corrections are small due to a strong nuclear field. The initial core state is calculated in a self-consistent potential including all electrons whereas the final electron state in the continuum is calculated in the potential of the ionized core. We use Eq. (6) to avoid problems with the orthogonality condition. For energies above 100 eV, there is practically no difference between the results obtained this way and those obtained when both initial and final states are calculated in the same potential. For smaller energies, however, the deviations are significant and use of more accurate potentials combined with Eq. (6) is important.

We computed the form factor Q assuming that outgoing electrons with any nonzero energy are detectable. However, current experiments can detect recoil electrons only with energy 1 keV or above (see, e.g., Ref. [33]). Thus, we also computed a reduced factor $\tilde{Q}$ that receives contributions only from those subshells that give rise to outgoing electrons with energy at least 1 keV. The result from this calculation for $\tilde{Q}$ may be directly used to interpret recent DM search results (see, e.g., Refs. [33,68]).

It is illustrative to compare the dimensionless factor $Q(\epsilon)$ for the ionization by a scalar particle with the dimensionless factor $K(\epsilon)$ of the axioelectric effect, defined via [56,69]

$$\sigma_a = (\epsilon_0/f_a)^2(c/v)K(\epsilon)a_0^2, \tag{9}$$

where σ_a is the axioelectric cross section and $\epsilon_0 = 27.21$ eV is the Hartree energy. As shown in Ref. [56], $K(\epsilon)$ is generally the largest when the energy of the incoming axion is large enough to excite the $1s$, $2s$, and $2p$ core electrons. In contrast, one observes from Fig. 2 that $Q(\epsilon)$ generally peaks for sub-keV scalar particles. This fact may be readily verified in the case of a massless axion and a massless scalar particle. Using Eq. (7) and the relation (see Ref. [52])

$$\sigma_a(m_a = 0)/\sigma_\gamma(\epsilon_\gamma = \epsilon) \approx \epsilon^2/(2\pi\alpha f_a^2) \tag{10}$$

(here ϵ is the axion energy), one obtains

$$Q(m = 0)/K(m_a = 0) \approx \epsilon_0^2/(2\epsilon^2), \tag{11}$$

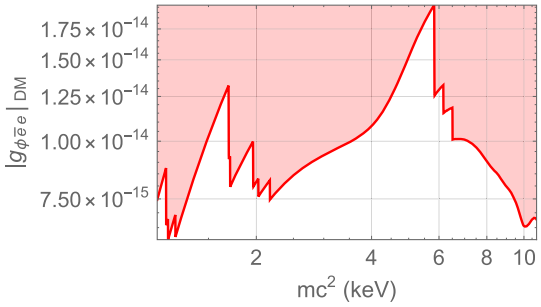

FIG. 3. Exclusion region for the $|g_{\phi\bar{e}e}|_{\rm DM}$ coupling strength as implied by Xenon1T experiment, assuming that the Xenon1T signal was caused by ionization by scalar dark matter.

which shows that at high energies $Q(\epsilon)$ is suppressed in comparison with $K(\epsilon)$. We tested the relation (11) numerically and found agreement within a few percent accuracy. The numerical data for the form factor K and its "cutoff" version $\tilde{K}$ are also presented in the Supplemental Material [53].

We now place limits on the electron-scalar coupling constant by assuming that the excess events recently recorded by the Xenon1T experiment [33] were a result of ionization by scalars.

We consider first the case in which the scalar particles saturate the local cold DM density $\rho_{\rm DM} \sim 0.3$ GeV/cm^3. In this case, the scalar flux is $\Phi_{\rm DM}^{\phi} = v\rho_{\rm DM}/(mc^2)$, where $v \sim 10^{-3}c$ and the expected ionization signal peaks at the scalar energy $\epsilon \approx mc^2$, with an event rate given by

$$R \approx \frac{4.8}{A}\frac{\tilde{Q}(m = \frac{\epsilon}{c^2})}{\text{year}}\left(\frac{g_{\phi\bar{e}e}}{10^{-17}}\right)^2\left(\frac{\text{keV}}{mc^2}\right)\left(\frac{M}{\text{ton}}\right), \tag{12}$$

where A is the average atomic mass number of the detector medium and M is the medium's total mass ($A \approx 131$ and $M = 1$ton for Xenon1T). Note that we have used the "cutoff" form factor $\tilde{Q}$ to account for the energy threshold of the detector.

The Xenon1T experiment reported an event rate of about 23.5/(ton × year) at around 2 keV. From the Supplemental Material [53], we have $\tilde{Q}_{\rm Xe}(\epsilon = mc^2 = 2\text{keV}) \approx 1.94 \times 10^{-3}$. Substituting these values into Eq. (12), we find that the Xenon1T result is consistent with

$$|g_{\phi\bar{e}e}|_{\rm DM} \approx 8.2 \times 10^{-15}, \tag{13}$$

assuming that it is caused solely by scalar DM. The Xenon1T result may also be interpreted as imposing a constraint on $|g_{\phi\bar{e}e}|$ for different scalar mass, as shown in Fig. 3.

Next, we consider the case in which the ionizing scalars are of solar origin, assuming $v \approx c$. Assuming that the dominant mechanisms for producing of solar scalars are the atomic recombination and deexcitation, Bremsstrahlung,

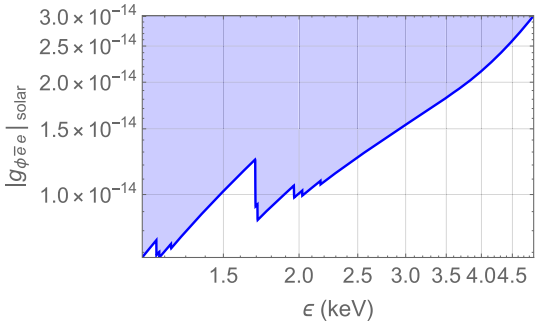

FIG. 4. Exclusion region for the $|g_{\phi\bar{e}e}|_{\rm solar}$ coupling strength as implied by the Xenon1T experiment, assuming that the Xenon1T signal was caused by ionization by solar scalar.

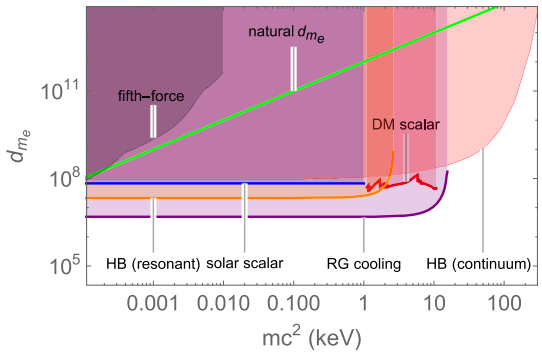

FIG. 5. Comparison of our limits on the electron mass modulus $|d_{m_e}|$ of scalar DM (thick red) and solar scalar (thick blue) implied by Xenon1T results with constraints from fifth-force searches (thin black) [72], red-giant cooling (thick purple), and horizontal-branch (HB) cooling (thick and thin orange) [73] and the naturalness argument (green) for a 10 TeV cutoff.

and Compton-like (ABC) processes, we estimate the solar scalar flux from solar opacity, as was done for axion in Ref. [70]. Using Eqs. (7) and (10), we write the ratio between the axion and scalar emission cross sections, and thus the corresponding fluxes, as

$$\Phi^{\phi}_{\rm solar}/\Phi^{a}_{\rm solar} = 2g^2_{\phi\bar{e}e}m_e^2/(g^2_{a\bar{e}e}\epsilon^2), \tag{14}$$

where $g_{a\bar{e}e} \equiv 2m_e/f_a$. Note that although we derived Eqs. (7), (10), and (14) for the case of bound-free electron transitions (ionization or recombination), they also hold for the cases of free-free (Bremsstrahlung and Compton-like processes) and bound-bound (deexcitation) transitions.

Redondo [70] gave, for $g_{a\bar{e}e} = 10^{-13}$, the value $\Phi^{a}_{\rm solar} \approx 0.95\times10^{20}/({\rm year\,m^2})$ at an incoming axion energy of 2 keV [71]. Using this value and Eq. (14), we write the rate of ionization by solar scalars as

$$R \approx \frac{8.3}{A}\frac{\tilde{Q}(m=0)}{\rm year}\left(\frac{g_{\phi\bar{e}e}}{10^{-15}}\right)^4\left(\frac{\rm keV}{\epsilon}\right)^2\left(\frac{M}{\rm ton}\right). \tag{15}$$

Substituting into Eq. (15) the Xenon1T event rate of $23.5/({\rm ton}\times{\rm year})$ and the value $\tilde{Q}_{\rm Xe}(m=0,\epsilon=2\ {\rm keV}) \approx 0.144$, one finds that the Xenon1T result is consistent with

$$|g_{\phi\bar{e}e}|_{\rm solar} \approx 1.0\times10^{-14}. \tag{16}$$

Using the dependence on ϵ of R [33], $\tilde{Q}(m=0)$ and the solar axion flux [70], we also derived limits on $|g_{\phi\bar{e}e}|_{\rm solar}$ as presented in Fig. 4.

We now compare the limits on $g_{\phi\bar{e}e}$ with those due to other DM searches and astrophysical observations. It is useful to convert from $g_{\phi\bar{e}e}$ to the electron mass modulus d_{m_e}, defined via

$$g_{\phi\bar{e}e} = \sqrt{4\pi}d_{m_e}m_e/m_P, \tag{17}$$

where $m_P \approx 1.22\times10^{19}$ GeV is the Planck mass. The constraint on $|d_{m_e}|_{\rm DM}$ may be inferred from that on $|g_{\phi\bar{e}e}|_{\rm DM}$ presented in Fig. 3. The constraint on $|d_{m_e}|_{\rm solar}$ may be inferred from that on $|g_{\phi\bar{e}e}|_{\rm solar}$ at a scalar energy 2 keV, where the Xenon1T signal is the strongest, yielding

$$|d_{m_e}|_{\rm solar} \le 6.8\times10^{7}. \tag{18}$$

Note that Eq. (18) is independent of the scalar mass m, as long as $mc^2 \ll \epsilon = 2$ keV.

Figure 5 shows constraints on $|d_{m_e}|$ alongside with those due to other scalar DM searches and astrophysical considerations. We see that the Xenon1T limits on $|d_{m_e}|_{\rm DM}$ and $|d_{m_e}|_{\rm solar}$ cut deep into the natural parameter space for a 10 TeV cutoff (the region below the green line). They are always better than fifth-force limits, are about an order of magnitude less stringent than the red-giant cooling limit, and are comparable with or better than horizontal-branch cooling limits.

One source of the observed excess rate in the Xenon1T experiment was attributed to the solar ABC axions [33]. Although the Xenon1T-derived constraints on the axion-electron coupling strength are a factor of 5–10 weaker than those from astrophysical analyses, Aprile *et al.* [33] argue that this tension could be relieved by underestimated systematic uncertainties in astrophysical analyses or estimates in solar fluxes (see, however, Ref. [34]). Since the ABC axion solar fluxes can be directly scaled to scalar fluxes [see Eq. (14)], we can draw a similar conclusion: the excess rate in Xenon1T can be also attributed to the solar scalars. As Fig. 5 shows, this interpretation is also in a similar tension with current astrophysical bounds. Finally, the scalar signal may also be detected by looking for diurnal and annual modulation in the same way as with solar axion and galactic dark matter.

We thank A. Arvanitaki for helpful discussions. This work was supported in part by the Australian Research Council Grants No. DP190100974 and No. DP200100150,

the Gutenberg Fellowship, and U.S. National Science Foundation Grant No. PHY-1912465. A. D. is grateful to the University of New South Wales for hospitality during his visit supported in part by the Gordon Godfrey fellowship.

[1] G. Angloher, A. Bento, C. Bucci, L. Canonica, A. Erb, F. von Feilitzsch, N. F. Iachellini, P. Gorla, A. Gütlein, D. Hauff *et al.* (CRESST Collaboration), Eur. Phys. J. C **74**, 3184 (2014).
[2] C. E. Aalseth, P. S. Barbeau, J. Colaresi, J. I. Collar, J. Diaz Leon, J. E. Fast, N. E. Fields, T. W. Hossbach, A. Knecht, M. S. Kos, M. G. Marino, H. S. Miley, M. L. Miller, J. L. Orrell, and K. M. Yocum (CoGeNT Collaboration), Phys. Rev. D **88**, 012002 (2013).
[3] E. Armengaud *et al.* (EDELWEISS Collaboration), J. Cosmol. Astropart. Phys. 05 (2016) 019.
[4] R. Bernabei, P. Belli, A. Bussolotti, F. Cappella, V. Caracciolo, R. Cerulli, C. J. Dai, A. D'Angelo, A. Di Marco, H. L. He, A. Incicchitti, X. H. Ma, A. Mattei, V. Merlo, F. Montecchia, X. D. Sheng, and Z. P. Ye, Universe **4**, 116 (2018).
[5] R. Agnese *et al.* (SuperCDMS Collaboration), Phys. Rev. Lett. **121**, 051301 (2018).
[6] E. Aprile *et al.* (XENON Collaboration), Phys. Rev. Lett. **121**, 111302 (2018).
[7] D. S. Akerib *et al.* (LUX Collaboration), Phys. Rev. Lett. **122**, 131301 (2019).
[8] Q. Wang *et al.* (PandaX-II Collaboration), Chin. Phys. C **44**, 125001 (2020).
[9] Y. Grossman and H. E. Haber, Phys. Rev. Lett. **78**, 3438 (1997).
[10] L. J. Hall, T. Moroi, and H. Murayama, Phys. Lett. B **424**, 305 (1998).
[11] A. Bottino, N. Fornengo, and S. Scopel, Phys. Rev. D **67**, 063519 (2003).
[12] A. Bottino, F. Donato, N. Fornengo, and S. Scopel, Phys. Rev. D **69**, 037302 (2004).
[13] C. Arina and N. Fornengo, J. High Energy Phys. 11 (2007) 029.
[14] D. G. Cerdeño, C. Muñoz, and O. Seto, Phys. Rev. D **79**, 023510 (2009).
[15] M. Kakizaki, E. K. Park, J. H. Park, and A. Santa, Phys. Lett. B **749**, 44 (2015).
[16] P. Ghosh, I. Lara, D. E. López-Fogliani, C. Muñoz, and R. Ruiz de Austri, Int. J. Mod. Phys. A **33**, 1850110 (2018).
[17] J. Preskill, M. B. Wise, and F. Wilczek, Phys. Lett. B **120**, 127 (1983).
[18] L. Abbott and P. Sikivie, Phys. Lett. B **120**, 133 (1983).
[19] M. Dine and W. Fischler, Phys. Lett. B **120**, 137 (1983).
[20] T. Mizumoto *et al.*, J. Cosmol. Astropart. Phys. 07 (2013) 013.
[21] V. Anastassopoulos *et al.* (CAST Collaboration), Nat. Phys. **13**, 584 (2017).
[22] A. Gattone *et al.*, Nucl. Phys. B, Proc. Suppl. **70**, 59 (1999).
[23] A. Morales *et al.*, Astropart. Phys. **16**, 325 (2002).
[24] R. Agnese *et al.* (SuperCDMS Collaboration), Phys. Rev. Lett. **112**, 241302 (2014).
[25] J. Hoskins, J. Hwang, C. Martin, P. Sikivie, N. S. Sullivan, D. B. Tanner, M. Hotz, L. J. Rosenberg, G. Rybka, A. Wagner, S. J. Asztalos, G. Carosi, C. Hagmann, D. Kinion, K. van Bibber, R. Bradley, and J. Clarke, Phys. Rev. D **84**, 121302(R) (2011).
[26] B. M. Brubaker, L. Zhong, Y. V. Gurevich, S. B. Cahn, S. K. Lamoreaux, M. Simanovskaia *et al.*, Phys. Rev. Lett. **118**, 061302 (2017).
[27] B. T. McAllister, G. Flower, E. N. Ivanov, M. Goryachev, J. Bourhill, and M. E. Tobar, Phys. Dark Universe **18**, 67 (2017).
[28] K. Ehret *et al.*, Phys. Lett. B **689**, 149 (2010).
[29] P. Pugnat *et al.* (OSQAR Collaboration), Phys. Rev. D **78**, 092003 (2008).
[30] A. S. Chou, W. Wester, A. Baumbaugh, H. R. Gustafson, Y. Irizarry-Valle, P. O. Mazur, J. H. Steffen, R. Tomlin, X. Yang, and J. Yoo, Phys. Rev. Lett. **100**, 080402 (2008).
[31] F. Della Valle, A. Ejlli, U. Gastaldi, G. Messineo, E. Milotti, R. Pengo, G. Ruoso, and G. Zavattini, Eur. Phys. J. C **76**, 24 (2016).
[32] S. J. Chen, H.-H. Mei, and W.-T. Ni, Mod. Phys. Lett. A **22**, 2815 (2007).
[33] E. Aprile *et al.* (XENON Collaboration), Phys. Rev. D **102**, 072004 (2020).
[34] L. Di Luzio, M. Fedele, M. Giannotti, F. Mescia, and E. Nardi, Phys. Rev. Lett. **125**, 131804 (2020).
[35] R. Bernabei, P. Belli, F. Montecchia, F. Nozzoli, F. Cappella, A. Incicchitti, D. Prosperi, R. Cerulli, C. J. Dai, H. L. He, H. H. Kuang, J. M. Ma, and Z. P. Ye, Int. J. Mod. Phys. A **21**, 1445 (2006).
[36] G. Aad *et al.*, Phys. Lett. B **716**, 1 (2012).
[37] A. Arvanitaki, J. Huang, and K. Van Tilburg, Phys. Rev. D **91**, 015015 (2015).
[38] K. Van Tilburg, N. Leefer, L. Bougas, and D. Budker, Phys. Rev. Lett. **115**, 011802 (2015).
[39] Y. V. Stadnik and V. V. Flambaum, Phys. Rev. Lett. **115**, 201301 (2015).
[40] Y. V. Stadnik and V. V. Flambaum, Phys. Rev. A **94**, 022111 (2016).
[41] A. Hees, J. Guéna, M. Abgrall, S. Bize, and P. Wolf, Phys. Rev. Lett. **117**, 061301 (2016).
[42] C. J. Kennedy, E. Oelker, J. M. Robinson, T. Bothwell, D. Kedar, W. R. Milner, G. E. Marti, A. Derevianko, and J. Ye, Phys. Rev. Lett. **125**, 201302 (2020).
[43] A. Arvanitaki, S. Dimopoulos, and K. Van Tilburg, Phys. Rev. Lett. **116**, 031102 (2016).
[44] P. W. Graham, D. E. Kaplan, J. Mardon, S. Rajendran, and W. A. Terrano, Phys. Rev. D **93**, 075029 (2016).
[45] A. Arvanitaki, P. W. Graham, J. M. Hogan, S. Rajendran, and K. Van Tilburg, Phys. Rev. D **97**, 075020 (2018).
[46] Y. V. Stadnik and V. V. Flambaum, Phys. Rev. Lett. **114**, 161301 (2015).
[47] Y. V. Stadnik and V. V. Flambaum, Phys. Rev. A **93**, 063630 (2016).
[48] A. A. Geraci, C. Bradley, D. Gao, J. Weinstein, and A. Derevianko, Phys. Rev. Lett. **123**, 031304 (2019).
[49] A. A. Geraci and A. Derevianko, Phys. Rev. Lett. **117**, 261301 (2016).
[50] Y. V. Stadnik and V. V. Flambaum, Phys. Rev. Lett. **113**, 151301 (2014).

[51] A. Arvanitaki, S. Dimopoulos, and K. Van Tilburg, Phys. Rev. X **8**, 041001 (2018).
[52] M. Pospelov, A. Ritz, and M. Voloshin, Phys. Rev. D **78**, 115012 (2008).
[53] See Supplemental Material at http://link.aps.org/supplemental/10.1103/PhysRevLett.127.081301 for a derivation of Eq. (3) and numerical results of calculations.
[54] A. Derevianko, O. Hemmers, S. Oblad, P. Glans, H. Wang, S. B. Whitfield, R. Wehlitz, I. A. Sellin, W. R. Johnson, and D. W. Lindle, Phys. Rev. Lett. **84**, 2116 (2000).
[55] We point out that a similar "orthogonality" condition also exists for the axioelectric effect, affecting the $L = 1$ multipole, as may be seen in Eq. (A18) in Ref. [56]. For axion energy of 1 keV and above, as was considered in Ref. [56], the $L = 1$ term is subleading and "orthogonality" has no significance. In the sub-eV region, however, it should be explicitly imposed to avoid numerical inaccuracy. The existence of the "orthogonality" condition also means that using free wave functions for the continuum also gives very wrong results.
[56] A. Derevianko, V. A. Dzuba, V. V. Flambaum, and M. Pospelov, Phys. Rev. D **82**, 065006 (2010).
[57] F. Wuilleumier, Phys. Rev. A **6**, 2067 (1972).
[58] W. Veigele, At. Data Nucl. Data Tables **5**, 51 (1973).
[59] G. Marr and J. West, At. Data Nucl. Data Tables **18**, 497 (1976).
[60] R. Bernabei, P. Belli, F. Cappella, V. Caracciolo, S. Castellano, R. Cerulli, C. J. Dai, A. d'Angelo, S. d'Angelo, A. Di Marco *et al.*, Adv. High Energy Phys. **2014**, 605659 (2014).
[61] J. Calvo, C. Cantini, P. Crivelli, M. Daniel, S. D. Luise, A. Gendotti, S. Horikawa, B. Montes, W. Mu, S. Murphy, G. Natterer, K. Nguyen, L. Periale, Y. Quan, B. Radics, C. Regenfus, L. Romero, A. Rubbia, R. Santorelli, F. Sergiampietri, T. Viant, and S. Wu, J. Cosmol. Astropart. Phys. 03 (2017) 003.
[62] E. Armengaud *et al.*, J. Cosmol. Astropart. Phys. 11 (2013) 067.
[63] C. E. Aalseth *et al.*, Eur. Phys. J. Plus **133** (2018).
[64] P. Adhikari *et al.* (DEAP Collaboration), Phys. Rev. D **102**, 082001 (2020).
[65] D. W. Amaral *et al.* (SuperCDMS Collaboration), Phys. Rev. D **102**, 091101 (2020).
[66] M. Antonello *et al.*, Astropart. Phys. **106**, 1 (2019).
[67] A. H. Abdelhameed *et al.*, Phys. Rev. D **100**, 102002 (2019).
[68] G. Adhikari *et al.*, arXiv:2104.03537.
[69] V. A. Dzuba, V. V. Flambaum, and M. Pospelov, Phys. Rev. D **81**, 103520 (2010).
[70] J. Redondo, J. Cosmol. Astropart. Phys. 12 (2013) 008.
[71] Inferred from the blue solid line in Fig. 6 in Ref. [70].
[72] E. Adelberger, B. Heckel, and A. Nelson, Annu. Rev. Nu cl. Part. Sci. **53**, 77 (2003).
[73] E. Hardy and R. Lasenby, J. High Energy Phys. 02 (2017) 033.